IOP Publishing Journal of Geophysics and Engineering
J. Geophys. Eng. **14** (2017) 502–512 (11pp) https://doi.org/10.1088/1742-2140/aa5f23

Experimental research on the ultrasonic attenuation mechanism of coal

Guanhua Liu[1,2], Zhentang Liu[1,2], Junjun Feng[1,2], Zuokun Song[3] and Zhenjing Liu[4]

[1] Key Laboratory of Gas and Fire Control for Coal Mines, Xuzhou, 221116, People's Republic of China
[2] Faculty of Safety Engineering, China University of Mining And Technology, Xuzhou, 221116, People's Republic of China
[3] Henan Province Energy Chemical Group Co., LTD, Yiyang Justice Network Coal Co., People's Republic of China
[4] Henan Province Energy Chemical Group Co., Hebi Coal Group, People's Republic of China

E-mail: Zhentang_Liu1@126.com

Received 12 June 2016, revised 14 December 2016
Accepted for publication 8 February 2017
Published 28 March 2017

Abstract

We studied the ultrasound velocity and attenuation coefficient in coal on the basis of acoustic emission analysis in the time and frequency domains. We also analyzed the mechanism of ultrasound attenuation in coal from a microscopic point of view. Previous research has indicated that the ultrasound velocity and the attenuation coefficient in coal correlate positively and negatively, respectively, with the coal density. In the present study, we found that the acoustic emission characteristics in the time and frequency domain are influenced by the quality of the coal and the fundamental frequency of the ultrasound. For example, the decay time was longer and the amplitude of the received signal was greater in anthracite than in fat coal. Moreover, with increasing fundamental frequency, the decay time decreased and the energy distribution in the transmitted wave became more concentrated around the fundamental frequency. In terms of energy dissipation, coal matrix deformation resulted in a pulling force and caused shear distortion owing to friction, the ultrasonic attenuation in coal is positively affected by the stress induced by ultrasonic waves, which means that a larger strain amplitude would lead to more energy dissipated in coal and an increase of the attenuation coefficient. This was the main cause of ultrasonic attenuation.

Keywords: ultrasonic wave, attenuation mechanism, time domain, frequency domain

(Some figures may appear in colour only in the online journal)

Nomenclature

v	Ultrasonic velocity	τ_f	Shear stress
l	Sample length	δ	Sliding displacement
t_1	Ultrasonic launching moment	σ	Compressive stress
t_2	Receiving moment	R	Crack constant
A_1	Amplitude of ultrasonic emission	C	Material constant
A_2	Reception amplitude	V_1 V_2	Poisson's ratio
α	Attenuation coefficient	E_1, E_2	Young's moduli
W_f	Friction energy	μ	Frictional coefficient
a	Contact length	θ	Included angle between crack and stress of ultrasound

1. Introduction

Understanding the nature of coal is necessary for preventing accidents in coal mines. The use of ultrasound to detect structural characteristics of rock is well established. Under certain conditions, ultrasound can be used to predict gas outbursts, probe the properties of dry coal and underwater coal (Wang *et al* 2015), and characterize internal defects and cracks in the coal surface (Xu *et al* 2015). Therefore, understanding the interaction between ultrasound and coal has important theoretical and practical significance in inverse modeling for coal geology.

In coal mine production, and in the application of ultrasonic parameters and characteristics of the coal and other aspects of ultrasound, domestic and foreign scholars have done a lot of research. Wang Yungang and coworkers showed semi-quantitatively in tectonic coal that the main factors that affect the longitudinal wave velocity and quality factor of the ultrasound are the porosity and volatility of the coal, and the moisture and ash content (Wang *et al* 2014). Li Tao and coworkers used ultrasound to identify the type of coal by constructing models to quantify the relationship between the coal structure and the ultrasonic velocity and attenuation coefficient. Using these models and a backpropagation neural network model, they were able to determine the type of coal structure (Li *et al* 2011). Zhai Xiaojie studied the ultrasonic properties of different types of coal under uniaxial compression (Zhai 2008). Xiao Xiaochun showed that, under high effective stress, ultrasound can improve the permeability of coal (Xiao *et al* 2016). In addition, Zhao determined that the capacity of coal to absorb methane and the rate of methane desorption are affected by ultrasound under isothermal conditions and also provided a theoretical explanation for this behavior (Zhao 2014).

Nondestructive ultrasound detection has been widely applied to study the internal structure of rocks. However, there are appreciable differences in the physical properties (in particular, the internal pore structure) between coal and rock; therefore, the ultrasonic attenuation mechanism of the rock cannot be directly applied to coal, and investigation of this in coal is necessary. To date, the mechanism of ultrasonic attenuation in coal is not clear. In this paper, we analyze the ultrasound parameters in two different coal samples in the presence and absence of stress, and from the results, draw preliminarily conclusions about the attenuation mechanism.

2. Experiment method

2.1. Sample preparation

We chose coal samples from two different coal mines; namely, from Sanhejian (SHJ) and Daanshan (DAS) coal mines, the locations of which are shown in figure 1(a). According to the ISRM recommended ultrasonic testing standard, the collected unified coal was drilled, cut, and ground to cylindrical samples 50 mm in diameter and 50 mm in length (figure 1(b)). At both ends, the sample roughness

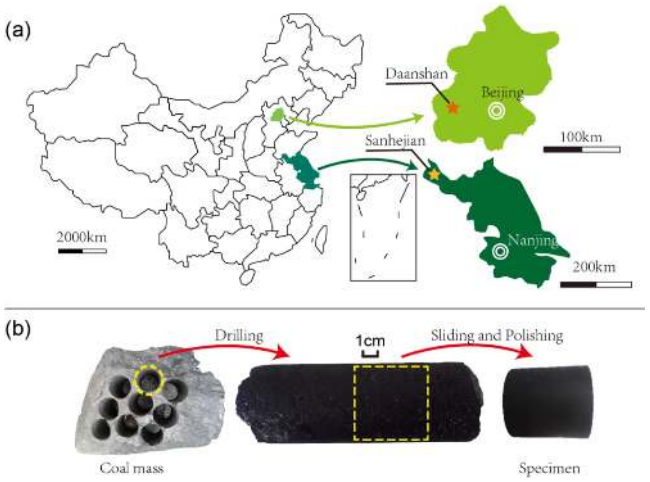

Figure 1. Coal sampling position and process.

was less than 0.02 mm, and the maximum deviation angle of the end face from the vertical axis was less than 0.25°. The finished coal samples are shown in figure 2.

The industrial analysis of Daanshan and Sanhejian sample specimen is as shown in table 1.

2.2. Experimental system

The experiments on ultrasonic transmission in coal use an ultrasonic experimental system, which mainly includes ultrasonic stimulating and receiving devices (Feng *et al* 2016). The experimental system is shown in figure 3. Ultrasound was generated using an ARB-1410 PCB instrument, which produces a high-frequency signal that is transmitted to the electrode plates of a crystal transducer, thus stimulating elastic vibrations of the piezoelectric crystal at the same frequency. When the transducer is coupled to a medium, the high-frequency elastic vibration will propagate through the medium. A multichannel ultrasonic receiver (Express-8) was used to measure the acoustic emission. The receiver used was a piezoelectric crystal, which produces an alternating charge when exposed to oscillating sound pressure. After the charge was converted to a voltage signal by the amplifier, it was delivered to the acoustic emission receiving channel. Finally, the ultrasound signal was visualized by the acoustic emission acquisition system. During the experiments, high-vacuum grease (designed especially for ultrasonic smear tests) was applied at both ends of the samples. The P-wave transducer was then bonded to the ends of the sample with a defined coupling force. The fundamental ultrasound frequency was 300 kHz, the initial amplitude was 150 V, and the receiving threshold was 45 dB.

The velocity of the transmitted wave, v, was calculated based on the transmitting time as follows:

$$v = \frac{l}{t_2 - t_1}, \tag{1}$$

where t_1 is the time at which the ultrasound is switched on, t_2 is the time at which the signal is received, and l is the sample length.

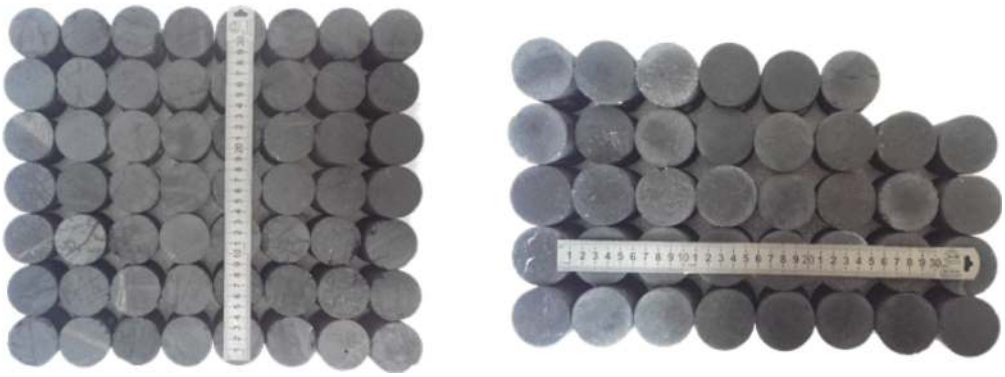

(a) Sanhejian sample (b) Daanshan sample

Figure 2. Photograph of processed coal sample.

Table 1. Results of proximate analysis on coal samples.

Sample code	Industry analysis				Coal types
	M_{ad} (%)	A_{ad} (%)	V_{da} (%)	FC_{ad} (%)	
SHJ	2.15	12.69	42.26	49.18	CYM
DAS	0.58	18.18	9.71	73.35	PM

The attenuation coefficient, l, was calculated based on the amplitude attenuation as follows:

$$\alpha = -[20\log_{10}(A_2/A_1)]/l, \quad (2)$$

where A_1 is the amplitude of ultrasonic emission and A_2 is the amplitude of the received signal.

3. Results

3.1. Effects of density

The elastic wave properties of rock are usually dependent on the rock's mineral composition and internal structure. Density is one of the most important properties of rock; thus, it is necessary to study the relationship between density, and the ultrasound velocity and attenuation coefficient. These relationships for the two coal samples are shown in figures 4 and 5. It can be seen that the density is positively correlated with velocity. The correlation between the density and attenuation coefficient is weak, but in general, with increasing density, the attenuation coefficient decreases.

3.2. Ultrasonic waveform time domain features

The spectral characteristics of an ultrasound wave that is transmitted through a coal sample depend of the physical properties on the sample. For example, when the scattering effect is relatively strong, there will be obvious tailing in the received signal. Because the amount of data acquired is too large to list, we have presented representative results for each sample in figures 6–11. The sampling frequency of each waveform file was 5×10^6 samples s^{-1} and the window length was 1.024 ms.

As shown figure 6, the initial ultrasonic waveform resembles a rectangular pulse. The transmitted waveform is still rectangular, albeit with a slight tail that is more pronounced in the DAS sample than in the SHJ sample. In addition, the transmitted waveform in the DAS sample is noisy, and the wave edge and first-motion waveform are clearer in the SHJ sample. In both samples, the amplitude reaches a maximum value quickly after the initiation of vibration, and then gradually decays. Using coda wave interferometry, the attenuation time of the signal in the DAS sample was found to be much longer than that in the SHJ sample. Moreover, this was longer when the coda wave was noisy. When the fundamental frequency was increased to 100 kHz (figure 7), the overall length of the signal in both samples increased substantially, and the high-frequency, noisy coda wave was almost absent. The length of the signal in the DAS sample was still longer than that from the SHJ sample, indicating that the elastic wave attenuation cycle in the DAS sample is longer than that of the SHJ sample. In addition, the signal in the SHJ sample was clearer than that in the DAS sample, and the amplitude quickly reached a maximum value before gradually decaying over time. When the frequency was increased to 200 kHz (figure 8), owing to the shorter duration of the emitted signal, the length of the transmitted signal in both samples was reduced SHJ and DAS, and the attenuation time was also substantially shortened. By contrast, the noisy and high-frequency coda wave began to appear in the tail of the transmitted signal in the SHJ sample; however, the duration of the high-frequency coda wave was still shorter than that in the DAS sample.

For a fundamental frequency of 300 kHz, the transmitted signal was further shortened. The signal can be divided into two parts: the body, which is cleaner and where the amplitude gradually decreases with time, and a high-frequency sine wave tail, which is particularly prominent in the DAS sample. In the tail, wavelets occupy about 50% of the overall signal. When the transmission frequency was further increased to 500 kHz, the transmitted signal was not only further reduced in length, but also the transmitted waveforms in the DAS and SHJ samples were no longer rectangular; rather, they were

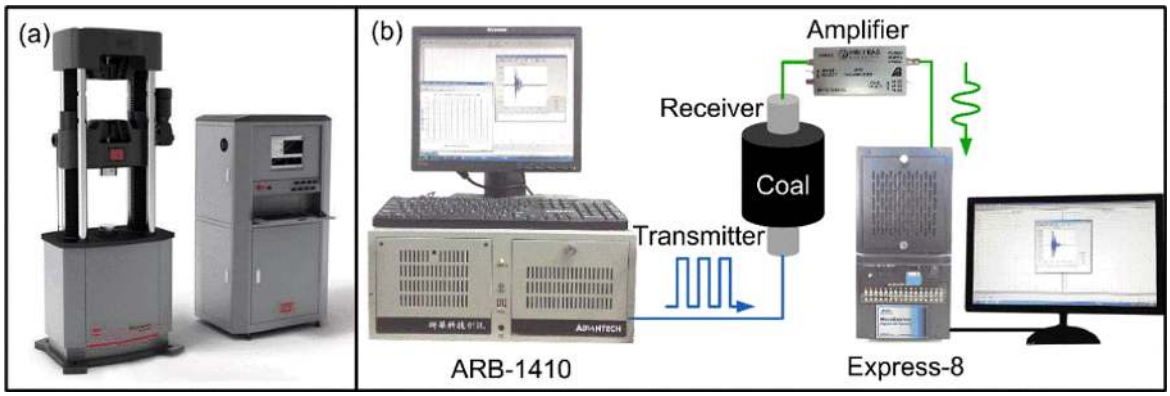

Figure 3. Schematic diagram of ultrasonic test system.

composed of high-frequency wavelets. The overall length of the signal was significantly smaller than that at 300 kHz. However, the duration of the transmitted signal in the DAS sample was still greater than that in the SHJ sample. Moreover, the length of the high-frequency noise was greater than in the SHJ sample. The first cycle in the SHJ sample was clearer than that in the DAS sample, and the amplitude reached a maximum value soon after transmission of the first ultrasound cycle. Finally, when the transmitter frequency was 700 kHz (figure 11), because the frequency was close to the resonant frequency of the transducer, the amplitude of the initial signal was weaker than that at lower frequencies. In this case, the head and tail of the transmitted signal contained relatively high-amplitude vibrations. The transmitted waveforms in the SHJ and DAS samples were not rectangular. In particular, for the DAS sample, the slower decay is indicative of elastic waves inside the sample.

3.3. Ultrasonic waveform frequency domain

In addition to the rich information contained in the time-domain spectra, the frequency-domain spectra also provided valuable information, allowing a more detailed analysis of attenuation. Typical ultrasound frequency spectra acquired for the two samples are shown in figures 12–17.

For a fundamental frequency of 50 kHz, as shown in figure 12, there is little difference between the transmitted signals in the two samples. The most dominant peak is at 250 kHz, with most other components almost completely absorbed by the coal medium. At a fundamental frequency of 100 kHz (figure 13), the transmitted signal comprises five main components, of which the peak at 100 kHz is the most dominant, followed by that at 250 kHz. For the transmitted signal in the SHJ sample, the amplitude of the peaks at 100 and 250 kHz is very similar. In addition, the maximum amplitude (5.43 V) of the DAS sample was significantly higher than that of the SHJ sample (1.71 V). For a fundamental frequency of 200 kHz (figure 14), the transmitted signal was dominated by the 200 kHz component. In this case, however, the transmitted signals of the two samples are markedly different from the initial ultrasound signal. Although the dominant frequency in the transmitted signals is 200 kHz, these waveforms contain many other components close to this frequency. That is, the energy is distributed more broadly after transmission.

When the fundamental frequency was increased to 300 kHz (figure 15), the energy of the transmitted signal was concentrated at 300 kHz, with other significant frequency components present. In addition, the maximum amplitude in the DAS sample (2.40 V) was significantly higher than that in the SHJ sample (1.30 V). When the fundamental frequency was further increased to 500 kHz (figure 16), the energy of the transmitted wave was mainly concentrated in the frequency range of 250–300 kHz, with the amplitude of the signal in the vicinity of 500 kHz being close to zero. This is attributed to the energy at the fundamental frequency being attenuated in the coal. The amplitude of the dominant frequency in the transmitted signal was higher in the DAS sample than in the SHJ sample. For a fundamental frequency of 700 kHz (figure 17), the amplitude of the transmitted signal at the fundamental frequency was reduced because of the large number of lower-frequency peaks that appear as a result of scattering. The transmitted signal contains almost no signal at frequencies above 500 kHz, with most energy concentrated around 300 kHz in the SHJ sample, and around 100–300 kHz in the DAS sample.

4. Media ultrasonic attenuation mechanism

Elastic wave attenuation of the rock materials has been widely studied, with particular focus on the effects of friction, fluid flow, viscous relaxation, and scattering (Lucet and Zinszner 1992). The attenuation usually results from a combination of two or more of these effects (Johnston *et al* 1979). Among those mechanisms, the effect of friction is considered the dominant mechanism of wave attenuation in dry rock under low confining pressure, and the internal sliding friction has been shown to only become significant when the rock is under low confining pressure and the strain is greater than 10^{-6} (Winkler *et al* 1979). The friction relates mainly to the energy dissipation induced by sliding on the contact surface of grains or cracks (Winkler and Nur 1982), which has been thoroughly discussed in the articles of Sharma and Tutuncu (Tutuncu *et al* 1998, 2016).

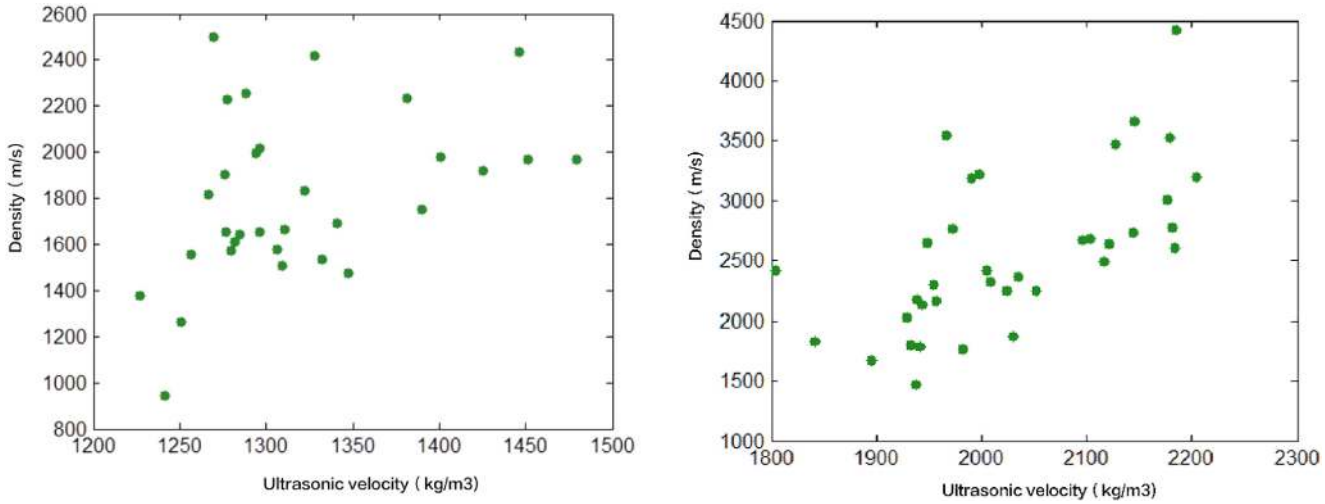

(a) SHJ (b) DAS

Figure 4. Relationship between wave velocity and density.

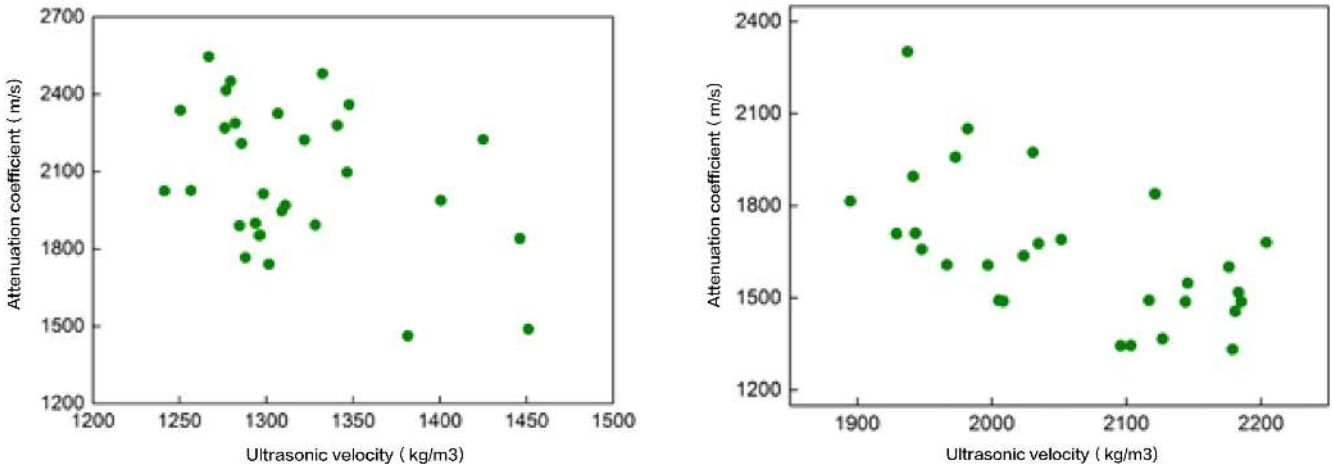

(a) SHJ (b) DAS

Figure 5. Relationship between attenuation and density.

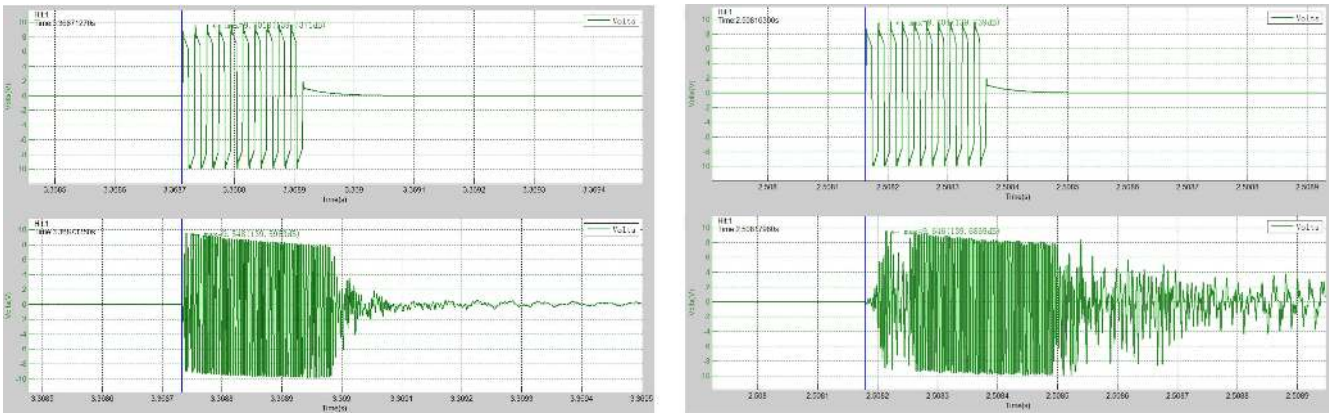

(a) SHJ (b) DAS

Figure 6. Wave transmitted and received at frequency of 50 kHz.

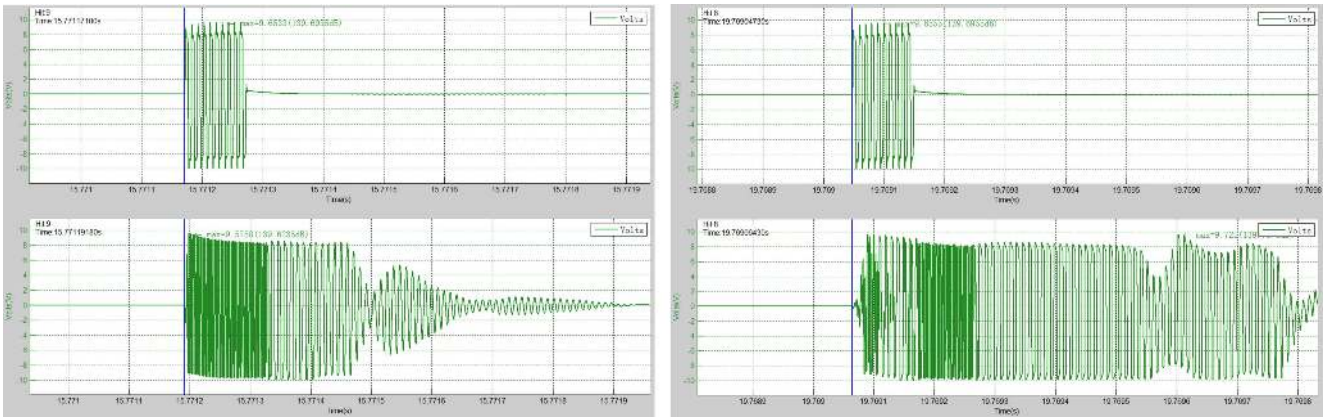

(a) Sanhejian Coalmine (b) Daanshan Coalmine

Figure 7. Wave transmitted and received at frequency of 100 kHz.

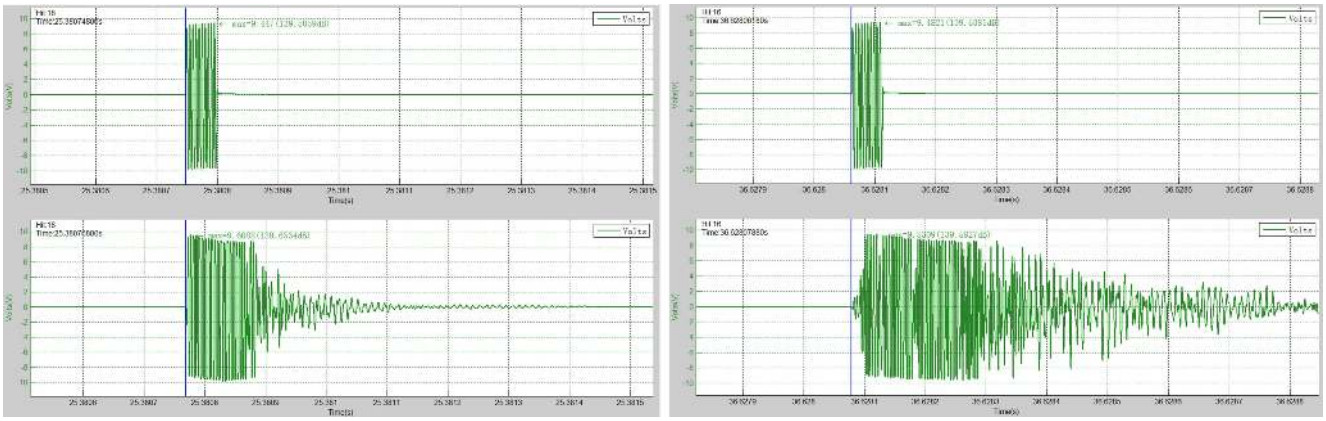

(a) Sanhejian Coalmine (b) Daanshan Coalmine

Figure 8. Wave transmitted and received at frequency of 200 kHz.

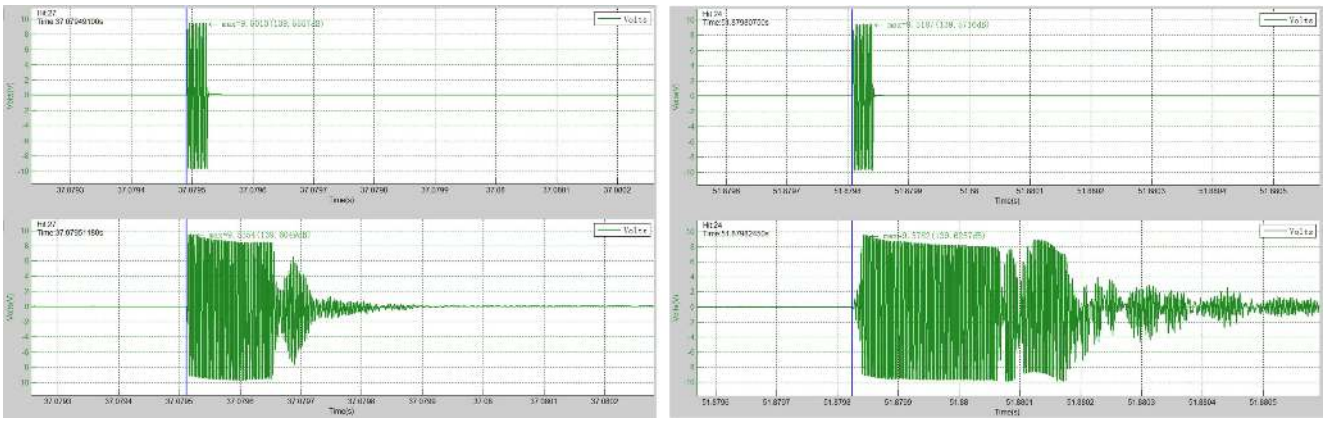

(a) SHJ (b) DAS

Figure 9. Wave transmitted and received at frequency of 300 kHz.

Coal is a typical rock material, thus the ultrasonic wave attenuation of coal in this study is also attributed to the effects of friction, fluid flow, viscous relaxation, and scattering. The effect of friction can be used to explain the influence of strain on the attenuation coefficient. External perturbations increase the relative motion of particles in the medium (Agioutantis 2016, Meng 2016). The dissipated energy, ΔW, is proportional to the relative sliding size of the particles, ΔU, and the sliding surface, S ($\Delta W \propto \Delta U \times S$). The relative sliding size is proportional to the strain amplitude (Walsh 1966, White 1966); thus, an increase of the strain amplitude will lead to an increase of the attenuation

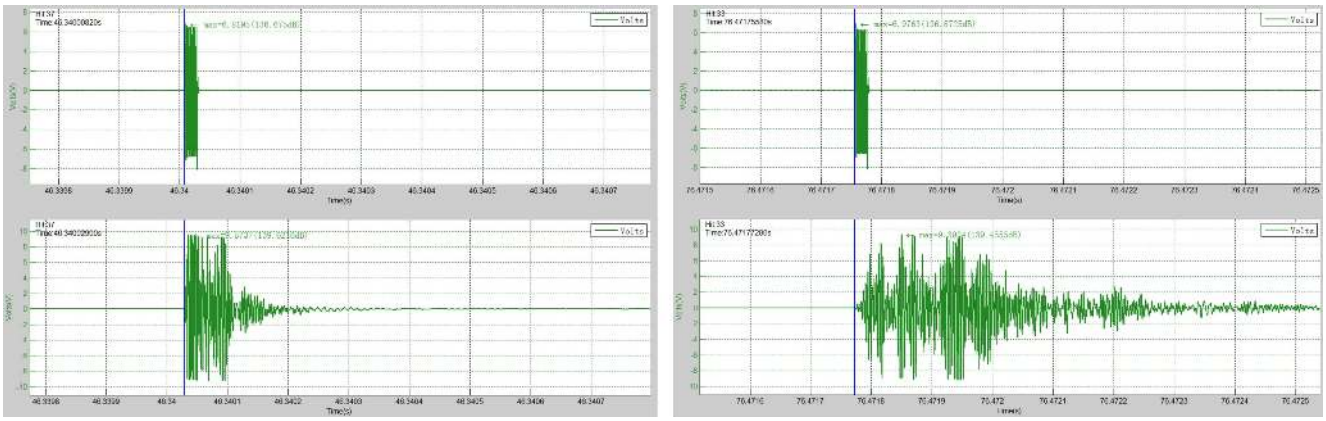

(a) SHJ (b) DAS

Figure 10. Wave transmitted and received at frequency of 500 kHz.

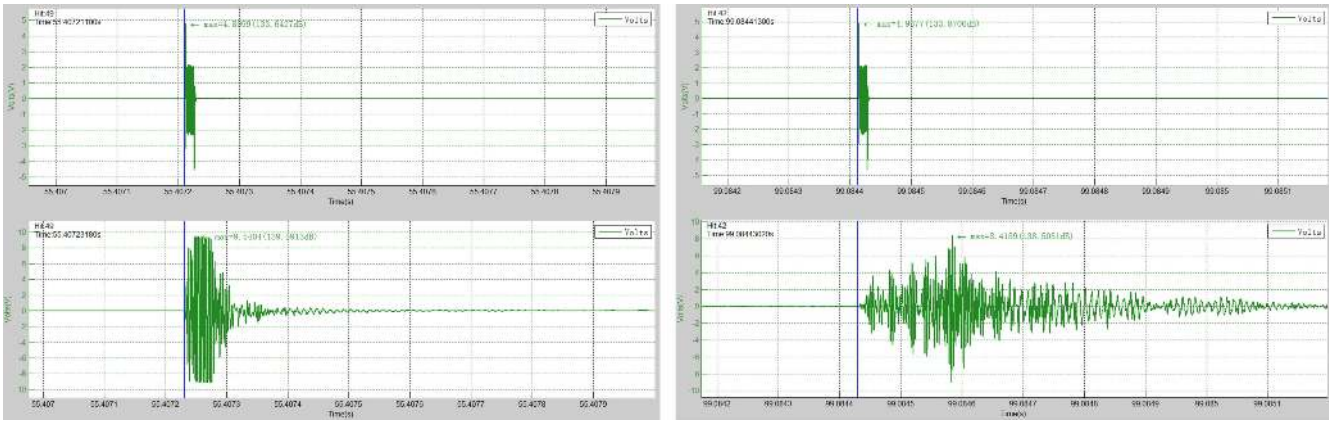

(a) SHJ (b) DAS

Figure 11. Wave transmitted and received at frequency of 700 kHz.

coefficient. In addition, the effect of confining pressure can be explained in terms of friction (Aydin 2014). A high confining pressure will act to close cracks in the rock, thereby suppressing fluid flow in the pores, and reducing the distance between the internal matrix and the fluid, which, in turn, reduces the attenuation coefficient (McCann and Sothcott 2009). Attenuation in the pore fluid is caused by friction from the relative motion of the pores, matrix, and fluid (Mavko and Amos 1979, Muller *et al* 2010, An *et al* 2006). The flow effect is the dominant attenuation mechanism of shock waves (1–1000 Hz) in porous media at the mesoscopic scale (i.e., on a scale larger than the pore size but smaller than the wavelength) (Tisato and Quintal 2013, Li *et al* 2014). Flow is caused by pressure differences in the fluid that arise from differences in fluid properties, and the density and contraction of the matrix (Quintal 2012). Viscous relaxation is caused by internal friction of the medium through stress relaxation (Jackson and Anderson 1970), and is therefore essentially related to the friction effect. Scattering, which attenuates ultrasound waves, is caused by grains in the solid medium and is prevalent when the grain size is similar to the wavelength. According to the ratio of the wavelength to the size of the heterogeneous body, the scattering effect can be classified as Rayleigh scattering, random scattering, or diffuse reflection (Mavko *et al* 2009). Because the grain size of typical rock is 0.1–1 mm and ultrasonic frequencies used in the laboratory are typically several hundred kilohertz, Rayleigh scattering is usually prevalent. In addition, according to the classification theory of Aki and Richard, when the wavelength is longer than the grain size, the medium can be regarded as an equivalent continuous medium and the attenuation caused by scattering can be ignored. Therefore, as to dry coal samples in this study, friction between the grain surface and cracks is considered to be main cause of shock-wave attenuation.

It should also be noted that the microstructure of coal is different from the sedimentary rock, such as sandstone. Sedimentary rock is usually composed of different mineral grains, and friction between the contact surfaces of these grains is the main mechanism of elastic wave attenuation. By contrast, for coal, the relative content of mineral grains is low and the attenuation is related with the porous structure of coal. The porous structure of coal is commonly analyzed using optical microscopy, transmission electron microscopy, field emission electron microscopy, and scanning electron microscope (SEM). In this paper, we used SEM to analyze the

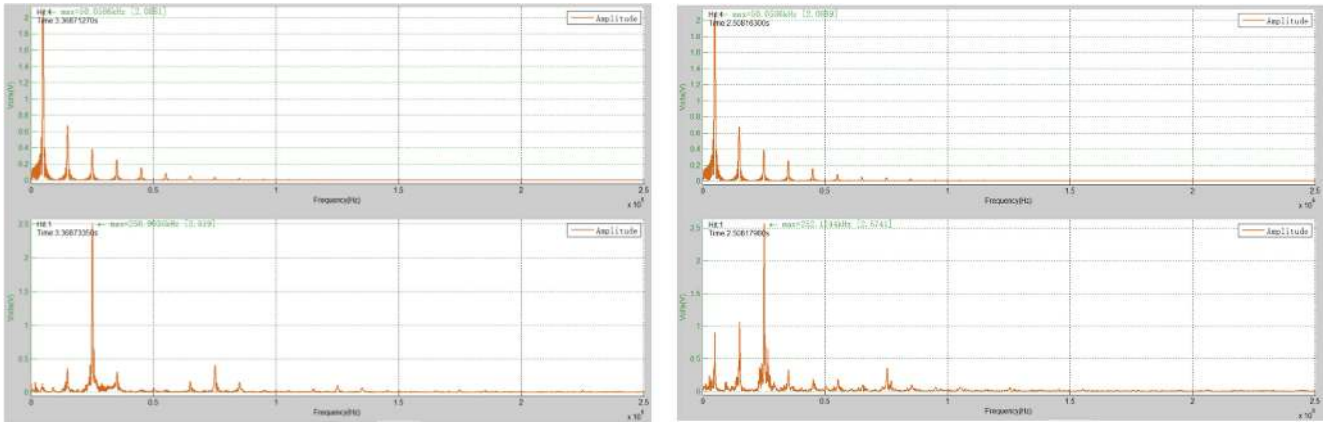

(a) SHJ (b) DAS

Figure 12. Wave spectrum transmitted and received at frequency of 50 kHz.

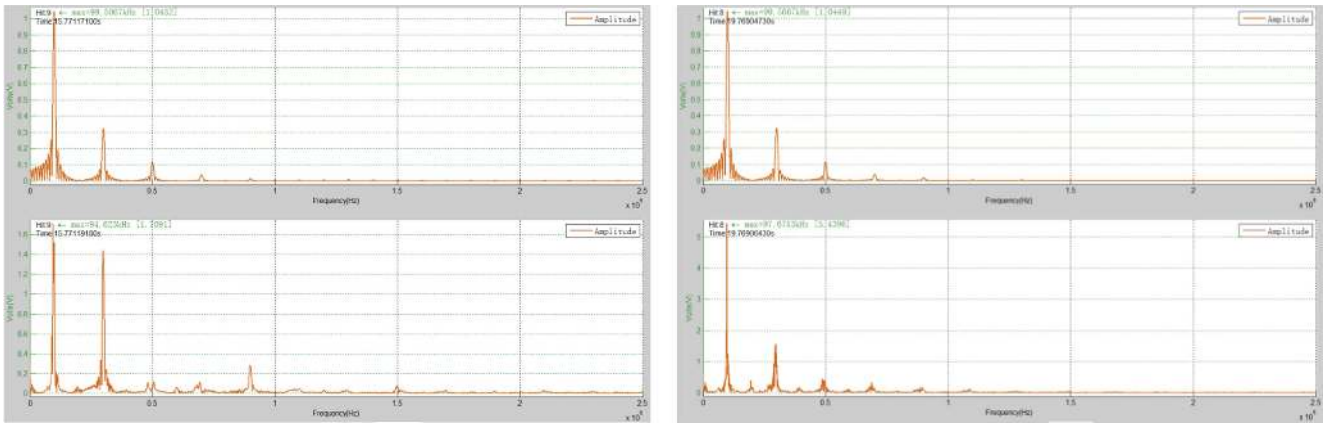

(a) SHJ (b) DAS

Figure 13. Wave spectrum transmitted and received at frequency of 100 kHz.

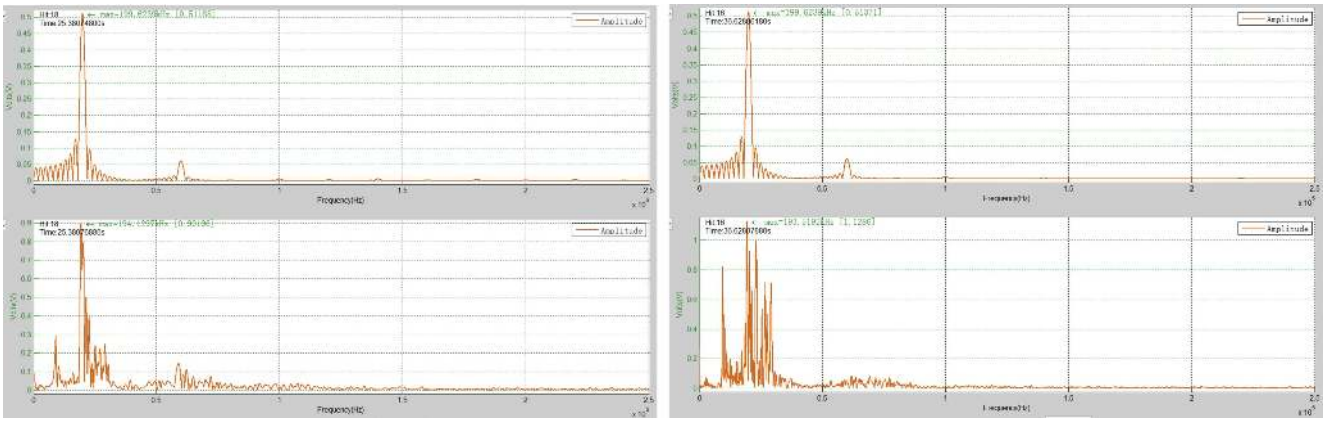

(a) SHJ (b) DAS

Figure 14. Wave spectrum transmitted and received at frequency of 200 kHz.

microstructures of the SHJ and DAS coal samples; the results are shown in figure 18. Consistent with previous descriptions of the porous structure of coal, we observed a large number of microscopic cracks and pores. Therefore, the friction between the crack surfaces and pore surfaces contributes to the major dissipated energy, ΔW, in coal.

According to elastic wave mechanics, ultrasonic waves cause slight tensile and compressive deformation within coal, and the friction occurs during the compressive deformation. The contact region between the crack surfaces and pore surfaces consists of several asperities that are in close proximity of each other, such as the grain contact model for sedimentary

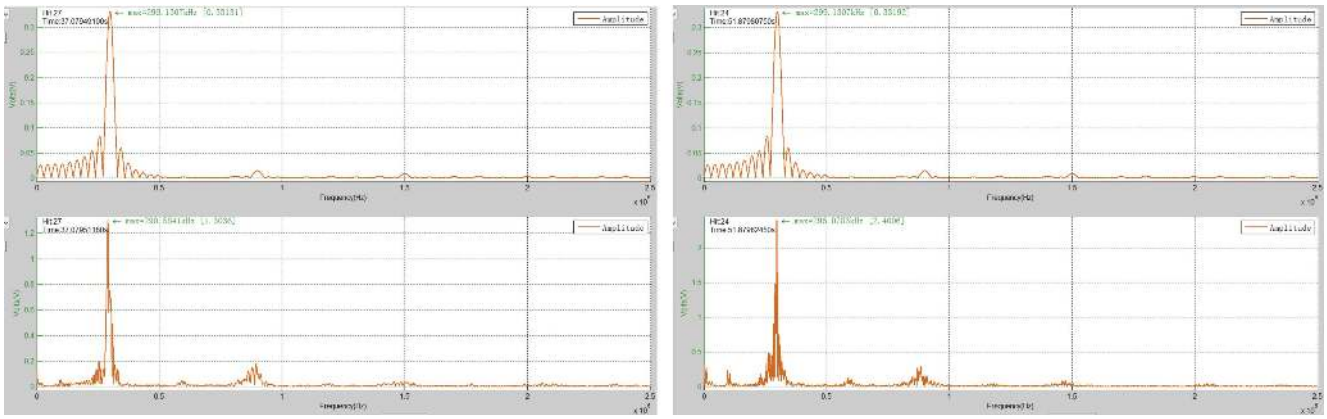

(a) SHJ (b) DAS

Figure 15. Wave spectrum transmitted and received at frequency of 300 kHz.

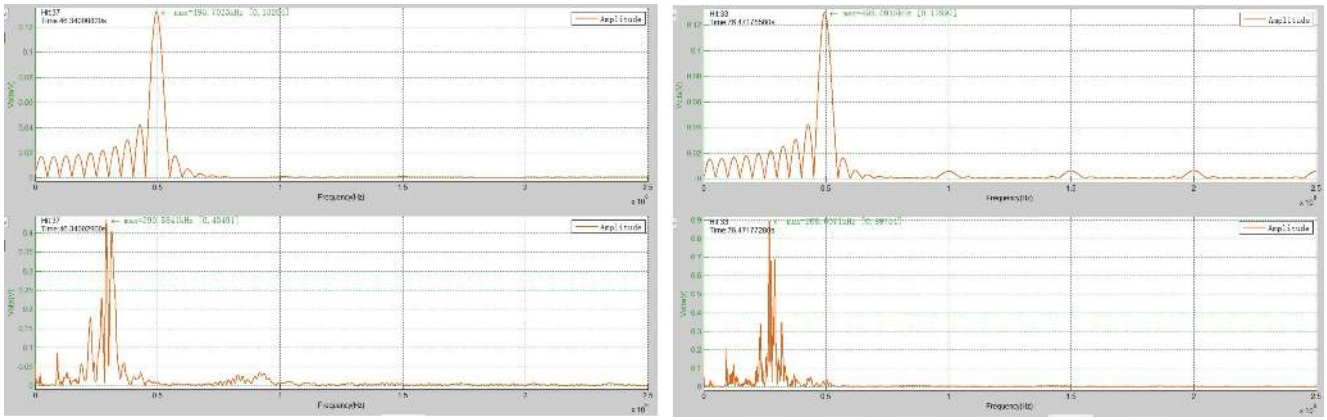

(a) SHJ (b) DAS

Figure 16. Wave spectrum transmitted and received at frequency of 500 kHz.

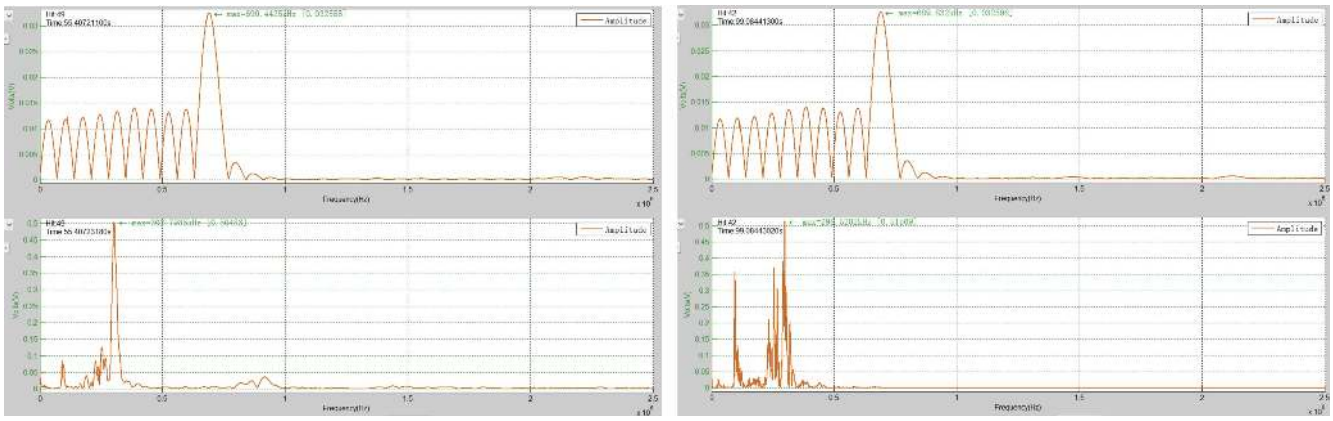

(a) SHJ (b) DAS

Figure 17. Wave spectrum transmitted and received at frequency of 700 kHz.

rock (Sharma and Tutuncu 1994). The energy dissipated in each asperity can be written as (Li *et al* 2000)

$$W_f = a\tau_f\sigma, \tag{3}$$

where τ_f is the shear stress on the initial crack surface caused by ultrasound, σ is the compressive stress, a is the contact length between the crack asperity shown in figure 19, and could be obtained by

$$a = 2 \times \left(\frac{3\pi}{4} \times RC\delta\right)^{\frac{1}{3}}, \tag{4}$$

where $R = R_1R_2/(R_1 + R_2)$, δ is the sliding displacement,

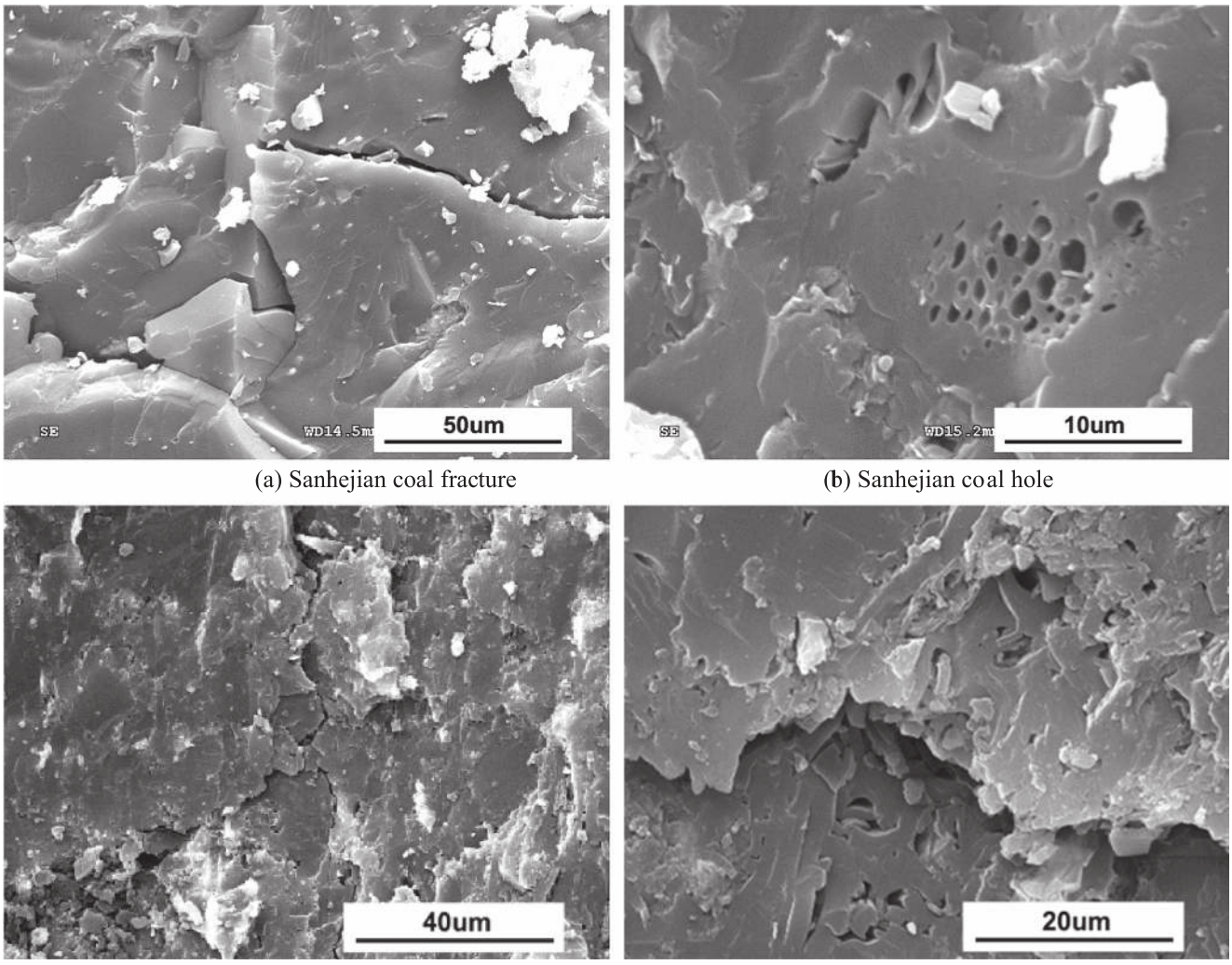

(a) Sanhejian coal fracture (b) Sanhejian coal hole

(c) Daanshan coal fracture (d) Daanshan coal hole

Figure 18. Micro-structure of coal obtained by SEM.

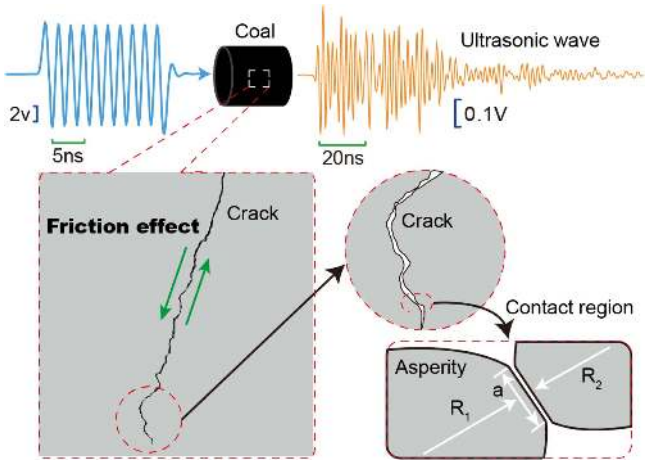

Figure 19. Schematic of ultrasonic attenuation of coal.

C is the material constant that can be written by:

$$C = \left[\frac{1 - V_1^2}{\pi E_1} + \frac{1 - V_2^2}{\pi E_2}\right], \tag{5}$$

where V_i and E_i represent Poisson's ratios and Young's moduli.

τ_f is

$$\tau_f = \frac{1}{2} \times \mu\delta(1 - \cos 2\theta), \tag{6}$$

where μ is the frictional coefficient and θ is the included angle between the crack and stress of ultrasound.

Based on equations (3)–(6), the ultrasonic attenuation in coal is positively affected by the stress induced by ultrasonic waves, which means that a larger strain amplitude would lead to more energy dissipated in coal and an increase of the attenuation coefficient.

5. Conclusion

(1) The ultrasonic velocity and attenuation coefficient of coal are related to the density of coal, ultrasonic velocity and density are substantially positively correlated and the velocity of waves becomes large as the

density increases; there is a correlation between the ultrasonic attenuation coefficient and density, as the density increases the attenuation coefficient shows a tendency to decrease.

(2) The temporal characteristics of ultrasonic attenuation in coal are related to coal quality, and the decay time is different in coal with different qualities; the decay time of anthracite coal is greater than fat coal, and with the improvement of the frequency of a wave, the decay time of the transmitted waveform is significantly reduced; the frequency domain characteristic in coal ultrasonic attenuation is also related to the quality of coal, and the frequency amplitudes are different with coal of different qualities, the amplitude frequency of anthracite is significantly greater than that of fat coal, and what's more, with the increasing of wave frequency, the energy of transmission waveform is gathered around the key waveform frequency more frequently.

(3) Based on the view of energy dissipation, the mechanism of ultrasonic attenuation in a matrix on different scales of the coal is caused by the crack friction effect which is aroused by tension–compression deformation, leading to the total mechanical energy elastic waves carry into heat energy, and ultimately ultrasonic attenuation appears. The ultrasonic attenuation in coal is positively affected by the stress induced by ultrasonic waves, which means that a larger strain amplitude would lead to more energy dissipated in coal and an increase of the attenuation coefficient.

Acknowledgments

This work is supported by the Research Project of Chinese Ministry of Education (No. 113031A), the National Natural Science Foundation of China (No. 51574231), the Outstanding Innovative Team of China University of Mining and Technology (No. 2014ZY001), and the Priority Academic Program Development of Jiangsu Higher Education Institutions (PAPD).

References

Agioutantis Z 2016 Potential of acoustic emissions from three point bending tests as rock failure precursors *Int. J. Min. Sci. Technol.* **01** 155–60

An Y, Mu Y and Fang C 2006 Relationship between attenuation, velocity of sedimentary rocks and petrophysical property *Oil Geophys. Prospect.* 188–92

Aydin A 2014 Upgraded ISRM suggested method for determining sound velocity by ultrasonic pulse transmission technique *Rock Mech. Rock Eng.* **47** 255–9

Feng J *et al* 2016 Experimental study of the stress effect on attenuation of normally *J. Appl. Geophys.* **132** 25–32

Jackson D D and Anderson D L 1970 Physical mechanisms of seismic-wave attenuation *Rev. Geophys.* **8** 1–63

Johnston D H, Toksöz M N and Timur A 1979 Attenuation of seismic waves in dry and saturated rocks: II. Mechanisms *Geophysics* **44** 691–711

Li H B, Zhao J and Li T J 2000 Micromechanical modelling of the mechanical properties of a granite under dynamic uniaxial compressive loads *Int. J. Rock Mech. Min. Sci.* **37** 923–35

Li T *et al* 2011 Study of the differentiating model for coal structure types based on BP neural network *Safety Coal Min.* 19–22

Li X B, Dong L G and Zhao Q 2014 Seismic modelling study of P-wave attenuation and velocity dispersion in patchy-saturated porous media *J. Geophys. Eng.* **11** 12

Lucet N and Zinszner B 1992 Effects of heterogeneities and anisotropy on sonic and ultrasonic attenuation in rocks *Geophysics* **57** 1018–26

Mavko G, Mukerji T and Dvorkin J 2009 *The Rock Physics Handbook: Tools for Seismic Analysis of Porous Media* (Cambridge: Cambridge University Press)

Mavko G M and Amos N 1979 Wave attenuation in partially saturated rocks *Geophysics* **44** 161–78

McCann C and Sothcott J 2009 Sonic to ultrasonic *Q* of sandstones and limestones: laboratory measurements at *in situ* pressures *Geophysics* **74** WA93–A101

Meng Q 2016 Numerical simulation study of the failure evolution process and failure mode of surrounding rock in deep soft rock roadways *Int. J. Min. Sci. Technol.* **26** 209–21

Muller T M, Gurevich B and Lebedev M 2010 Seismic wave attenuation and dispersion resulting from wave-induced flow in porous rocks—a review *Geophysics* **75** A147–64

Quintal B 2012 Frequency-dependent attenuation as a potential indicator of oil saturation *J. Appl. Geophys.* **82** 119–28

Sharma M M and Tutuncu A N 1994 Grain contact adhesion hysteresis: a mechanism for attenuation of seismic waves *Geophys. Res. Lett.* **21** 2323–6

Tisato N and Quintal B 2013 Measurements of seismic attenuation and transient fluid pressure in partially saturated Berea sandstone: evidence of fluid flow on the mesoscopic scale *Geophys. J. Int.* **195** 342–51

Tutuncu A N, Katsuki D, Padin A, Bui B and McDowell B 2016 Coupling geomechanics and petrophysical measurements for production enhancement in organic-rich shales *Unconventional Resources Technology Conference (San Antonio, TX 1–3 August)* URTEC-2461986-MS

Tutuncu A N, Podio A L, Gregory A R and Sharma M M 1998 Nonlinear viscoelastic behavior of sedimentary rocks: I. Effect of frequency and strain amplitude *Geophysics* **63** 184–94

Walsh J B 1966 Seismic wave attenuation in rock due to friction *J. Geophys. Res.* **71** 2591–9

Wang Y *et al* 2014 Analysis on influence factors of ultrasonic parameters for tectonic coal *J. Safety Sci. Technol.* **10** 82–6

Wang Y *et al* 2015 Experimental study on ultrasonic wave characteristics of coal samples under dry and water saturated conditions *J. China Coal Soc.* **40** 2445–50

White J E 1966 Static friction as a source of seismic attenuation *Geophysics* **31** 333–9

Winkler K, Nur A and Gladwin M 1979 Friction and seismic attenuation in rocks *Nature* **277** 528–31

Winkler K W and Nur A 1982 Seismic attenuation: effects of pore fluids and frictional sliding *Geophysics* **47** 1–15

Xiao X *et al* 2016 Coal rock microscopic damage evolution model and permeability increase mechanism research under ultrasound *Nat. Gas Geosci.* **10** 166–72

Xu X *et al* 2015 Effect of coal and rock characteristics on ultrasonic velocity *J. China Coal Soc.* **40** 793–800

Zhai X 2008 *Ultrasonic Properties of Rock Under Uniaxial Loading* (Sichuan: Chengdu University of Technology)

Zhao L 2014 *Physical Simulation Permeability Enhancement Coals Under Wave Action* (Jiangsu: University of Mining and Technology)